Heating rate effects on the crystallization behavior of isotactic polypropylene from mesophase – A de-polarized light transmission study

AUTHOR(S):

Asakawa, Harutoshi; Nishida, Koji; Yamamoto, Junpei; Inoue, Rintaro; Kanaya, Toshiji

CITATION:

Asakawa, Harutoshi ...[et al]. Heating rate effects on the crystallization behavior of isotactic polypropylene from mesophase – A de-polarized light transmission study. Polymer 2012, 53(13): 2777-2782

ISSUE DATE:

2012-06

URL:

http://hdl.handle.net/2433/157233

Heating rate effects on the crystallization behavior of isotactic polypropylene from mesophase – A de-polarized light transmission study

Harutoshi Asakawa, Koji Nishida*, Junpei Yamamoto, Rintaro Inoue, and Toshiji Kanaya

Institute for Chemical Research, Kyoto University, Uji, Kyoto, 611-0011, Japan

---

Corresponding author. Tel.: +81 774 38 3141; fax: +81 774 38 3146.

E-mail address: knishida@scl.kyoto-u.ac.jp (K. Nishida).

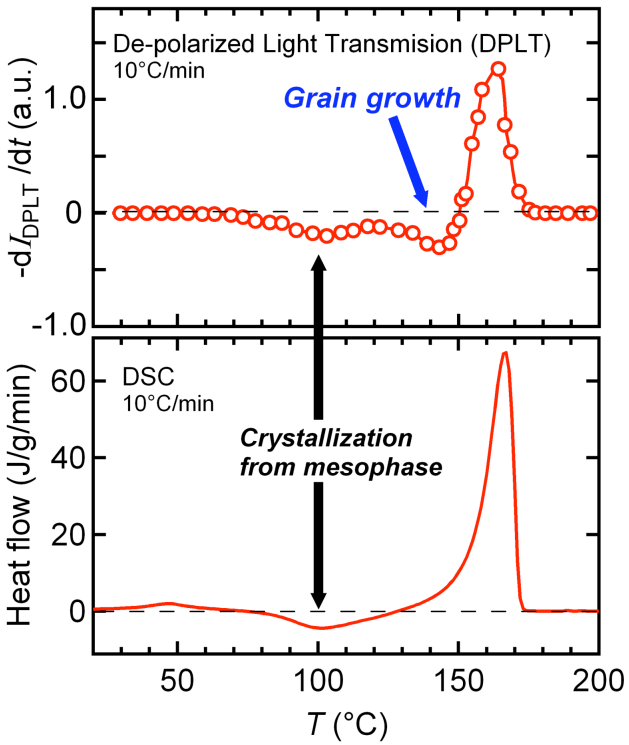

Graphical Abstract

ABSTRACT

It was ever reported in a communication of this journal that the large crystal grains having "bamboo leaf-like (BL)" morphology were produced by a rapid heating of isotactic polypropylene (iPP) from the mesophase. In order to optimize the condition to generate the BL crystals, heating rate effects on the crystallization behavior from the mesophase of iPP have been studied by utilizing a de-polarized light transmission (DPLT) method. The DPLT sensitively detected not only the cold crystallization from the mesophase around 100–120 °C but also the crystal grain growth in a narrow temperature region just below the melting temperature. With increasing the heating rate, both the temperature regions of the cold crystallization and the crystal grain growth shifted toward the higher temperatures. When the heating rate is slow (< 20 °C/min), the crystal grain growth was not conspicuous. With increasing the heating rate, the rate of the crystal grain growth increased and showed a maximum when the heating rate is approximately 60–80 °C/min. However, excessively fast heating (> 100 °C/min) also suppressed the crystal grain growth.

Keywords

isotactic polypropylene (iPP)

mesophase

de-polarization light transmission (DPLT)

1. Introduction

Crystallization of polymer in bulk usually results in the formation of spherulite, the diameter of which often reaches into several tens micrometer. The spherulite is not a single crystal; namely it consists of both crystalline lamellae and non-crystalline amorphous regions. In a spherulite a large number of the lamellae grow radially accompanied by occasional branching from a central nucleus [1]. The amorphous regions are inserted between the lamellae with a certain periodicity. Therefore the size of a crystal grain, which can be regarded as a single crystal, is far smaller than the diameter of a spherulite. Isotactic polypropylene (iPP) is no exception and it produces the spherulite when crystallized from the molten state [2]. Whereas we have ever found that the large crystal grains of several tens micrometer having “bamboo leaf-like (BL)” morphology were produced by annealing subsequent to rapid heating from the mesophase of isotactic polypropylene (iPP) [3,4].

The “mesophase” as the initial state must be essential for this particular crystallization, because the crystallization from an isotropic melt just results in the formation of spherulite as mentioned previously. However, the role of the mesophase in this particular crystallization is still unsolved. The mesophase iPP is obtained by quenching molten amorphous iPP into less than approximately 35 °C [5,6]; usually this is achieved by dropping a thin piece of iPP rapidly into ice water [7]. The chain conformation in the mesophase iPP is the regular 3/1 helices of the isotactic chain configuration as well as the cases in the crystalline phases, such as the alpha-, beta- and gamma-forms [8]. On a crystallographic scale, the lateral chain arrangement in the mesophase iPP is less ordered than that in the crystalline phases but much

better than that in the amorphous, as was characterized by two broad peaks in wide-angle X-ray diffraction (WAXD) pattern [9]. In conformity with the local structure, the level of stabilization energy of the mesophase iPP is also intermediate between that of amorphous and crystalline. Specifically the enthalpy of fusion of the mesophase iPP is approximately 75 % of the alpha-form crystal [10]. On a mesoscopic scale, the mesophase iPP is cellulated into the granular particles, so-called "nodules" with a diameter of approximately 10 nm, as was revealed by small-angle X-ray scattering (SAXS), transmission electron microscopy (TEM) and atomic force microscopy (AFM) [11-15]. Above the mesoscopic scale, no characteristic structure has so far been reported, except for the transient fluctuations in micrometer order during the formation of the mesophase [6]. This should be the major reason for the macroscopic transparency of the mesophase iPP.

The "rapid heating" in the crystallization process should be also deeply associated with the generation of the BL crystal, because a cold crystallization from the mesophase of iPP with a slow heating just resulted in the formation of the nodular crystallites [14], although the diameter of which became somewhat larger than that of the original mesophase. Most of the studies, which aimed at the heating rate effects on the cold crystallization behavior from the mesophase iPP, have so far been conducted using a differential scanning calorimetry (DSC) [16]. During a slow heating scan measured by a conventional DSC (10 °C/min), a shallow exotherm peak due to the cold crystallization (T_x) was observed around 100 °C and an endotherm peak due to the melting (T_m) was observed around 165 °C [10]. With increasing the heating rate, the T_x and T_m shifted toward the higher and the lower temperatures,

respectively. Eventually, the mesophase of iPP melted without occurring the cold crystallization when the heating rate exceeded 10^4 °C/s, as was revealed by an ultra fast DSC technique [17]. Thus, the DSC technique sensitively detected the crystallization and melting during the heating process up to an extremely fast rate, however, it does not tell anything about the morphology. On the other hand, from a structural point of view, *in situ* measurements for the crystallization from the mesophase iPP during slow or stepwise heating and also *ex situ* measurements for the quenched sample after heating have been performed by WAXD, SAXS, TEM and AFM [11-14]. The results of these structural studies with slow heating have established the concept that the cold crystallization from the mesophase of iPP resulted in the formation of the nodular crystallites, as was mentioned previously. Since structural measurements, such as WAXD, SAXS, AFM, etc., generally require longer data acquisition time than the DSC measurements, those techniques have not been applied to the fast heating process.

In the present study, we have applied a de-polarized light transmission (DPLT) method to investigate the crystallization of iPP from the mesophase. The DPLT method usually gives similar information to the DSC [18], because it is sensitive to the change in the degree of birefringence and the birefringence depends on the crystallinity. In fact, the DPLT has another advantage; the intensity of the DPLT is very sensitive to the size of the crystal grain even if the crystallinity is unchanged. Furthermore the DPLT requires only a short data acquisition time. This is the merit essential to apply the technique to the observation during fast scanning of temperature. As it will turn out later, these characteristics of the DPLT are especially useful

to study the crystallization of iPP from the mesophase. In order to validate the characteristics of the DPLT measurements, the data obtained by the DPLT is compared with those obtained by the established methods, such as DSC, WAXD, and SAXS on the same heating condition. Combinatorial application of multiple methods synergistically helps us understand the polymer crystallization [19].

2. Experimental section

2.1. Materials and sample preparations

The iPP material was supplied from Idemitsu Unitech Co., Ltd; the weight-average molecular weight was M_w = 353000, with a polydispersity of M_w / M_n = 4.4, and a degree of isotacticity (a meso pentad value) of *mmmm* = 0.98. This isotacticity is greater than the critical value (0.68) of isotacticity required to form the mesophase [20]. Sample films 200 μm-thick were prepared by quenching molten iPP to 0 °C by dipping them into ice water. Thus prepared films showed two broad peaks in WAXD pattern.

2.2. Hot stage with constant heating rates

Sample films of the mesophase iPP were heated from room temperature to 200 °C with various heating rates using a laboratory-made hot stage. The hot stage consisted of a heater block and a control unit. The heater block has a similar construction to the one that was previously used in a temperature jump experiment [6]. The control unit was assembled combining a programmable CPU unit KV-3000 and a PID temperature control unit KV-TF40,

products of KEYENCE Japan. With increasing the heating rate, the temperature at the sample position tended to delay in comparison to the programmed one; therefore the heating rates were calibrated for each case using the actually measured temperature at the sample position. Accordingly, the values of the heating rate indicated in the results are not round numbers. The range of the heating rate after calibration covered from 10 to 124 °C/min.

2.3. De-polarized light transmission (DPLT) measurements

The intensity of the light transmitted through the sample film was measured by utilizing the direct beam monitoring optics of a high-resolution small-angle light scattering instrument [21] with a diode laser of wavelength 405 nm as the light source. Utilization of this particular optics is efficient to measure the transmitted light at a good signal-to-noise ratio by suppressing the contamination of scattered light. A polarizer and an analyzer were inserted before and after the sample. By combination with a wide-dynamical range photometer, the measured intensity of transmitted light covered five orders of magnitude. The measuring time of the photometer was 0.2 s and the temperature error caused by this measuring time is approximately 0.4 °C in the case of the fastest heating rate (124 °C/min) of the present study.

The intensity of the DPLT (I_{DPLT}) through a film, whose areal size is larger than the cross-section of light beam, is given by the following relation;

$$I_{DPLT} \sim \sin^2(\pi \Gamma/\lambda) \qquad (1)$$

where Γ and λ are optical retardation and wavelength of light, respectively. The optical retardation Γ is a product of thickness of the film d and index of birefringence Δn. By analogy, I_{DPLT} for a case of dispersed cubic particles, whose dimension on a side is also d, is given by the following relation;

$$I_{\mathrm{DPLT}} \sim NS \sin^2(\pi d\Delta n/\lambda) \qquad (2)$$

where N and S are number of particle and cross-sectional area of a particle ($= d^2$), respectively. In this case, a certain fraction of particles, whose relative orientation to the light beam fulfills the condition to produce the birefringence, can contribute to the intensity. When the value of $d\Delta n/\lambda$ is small enough, equation (2) can be approximated as follows;

$$I_{\mathrm{DPLT}} \sim Nd^4\Delta n^2. \qquad (3)$$

The equation (3) tells that the DPLT is very sensitive to the size of a birefringent particle through the term d^4; *e.g.*, the value of I_{DPLT} becomes twice when the size of a particle becomes twice on the condition that the total volume of the particles and Δn are constant. It should be noted that equation (3) and the explanation for it are only the initial characteristics of equation (2) for small $d\Delta n/\lambda$; *e.g.*, $d\Delta n/\lambda <$ ca. 0.15. With approaching $d\Delta n/\lambda$ to 0.5, the value of equations (2) reaches a ceiling and oscillates ($d\Delta n/\lambda > 0.5$). Therefore any discussion, even qualitatively, becomes completely invalid for $d\Delta n/\lambda > 0.5$. For confirmation we performed a

polarization microscope observation for the sample, which showed the largest value of I_{DPLT} in the present study. The obtained image just showed dark grayish color, meaning that the value Γ is less than approximately 150 nm. Since the wavelength of light for the DPLT measurement is 405 nm, the value Γ/λ (= $d\Delta n/\lambda$) is estimated to be 0.37 at most; namely it is a safe side of 0.5. However, it should be noted again that the value of I_{DPLT} tends to become less sensitive with approaching $d\Delta n/\lambda$ to 0.5.

2.4. Complemental measurements

The DPLT has an above-mentioned detection property for a hypothetical system that consists of cubic birefringent particles. However, its application to the particular crystallization of iPP has not been established yet. The validation of the DPLT method is performed by comparing with the data obtained by the established methods.

In order to get structural information on a mesoscopic scale, SAXS measurements were performed. The measurements were conducted using X-ray beam lines BL40B2 and BL03XU in a synchrotron radiation (SR) facility, SPring-8, Hyogo, Japan. In the present measurements, the wavelength of the incident X-ray λ was selected to 1.0 Å. The scattering vector q (= $4\pi \sin\theta / \lambda$) was covered from 0.07 to 2.0 nm^{-1}, where θ is a half of the scattering angle (2θ). After standard data processing, such as correcting detector sensitivity and subtracting scattering from the empty sample cell, the data were circularly averaged, because the 2D-data showed no anisotropy. The DPLT data were also compared with DSC and WAXD data that were taken on the same heating condition in a previous work [10].

3. Results and discussion

3.1. Comparison of DPLT with other methods

The present crystallization study was performed during non-isothermal heating processes. The DSC is one of the standard methods among the non-isothermal measurements. Therefore the data obtained by other methods, including the DPLT, are displayed in reference to the DSC's. In the non-isothermal DSC, the observed enthalpy ΔH as a function of temperature T is displayed in the form of a heat capacity $\mathrm{d}(\Delta H)/\mathrm{d}T$ or a heat flow $\mathrm{d}(\Delta H)/\mathrm{d}t$. Since the rates of structure formation will be discussed in this study, the DSC was handled in the form of the heat flow. The relation between the heat capacity and the heat flow is given by as follows;

$$\mathrm{d}(\Delta H)/\mathrm{d}t = \mathrm{d}(\Delta H)/\mathrm{d}T \times \mathrm{d}T/\mathrm{d}t. \qquad (4)$$

It is a matter of preference; we took the positive side of the DSC chart as the endothermic and the negative side exothermic. Accordingly, also for other methods, the observed quantities were converted into the differential form and the rates of structure formations were displayed in the negative values when the data obtained by different methods are compared. The comparison was performed for the data obtained at a heating rate of 10 °C/min.

Figure 1 shows a DPLT measurement, I_{DPLT} as a function of T, observed at a heating rate of 10 °C/min. At room temperature the I_{DPLT} showed a small but somewhat larger value than that of the isotropic molten state (see, $T > 175$ °C). This is because the mesophase iPP has

locally a liquid crystal-like order although it is cellulated into the nodular domains. With increasing the temperature, the I_{DPLT} also increased showing two steeply increasing temperature regions around 100 and 145 °C, eventually it decreased very steeply around 165 °C. The steep decrease is unquestionably assigned to the melting of crystal. The interpretation for the two steep increases will be discussed later in the differential form referring the data obtained by other methods.

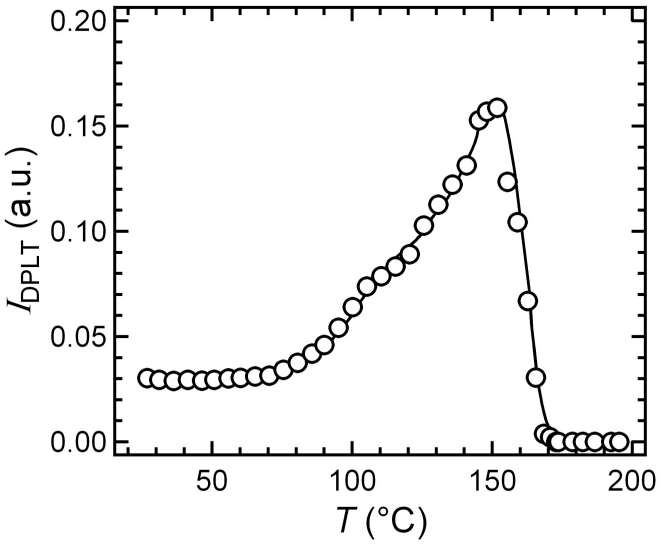

Fig. 1. DPLT intensity I_{DPLT} as a function of temperature T, measured at a heating rate of 10 °C/min.

The observed I_{DPLT} as a function of T was converted into the differential form similarly to equation (4) as follows;

$$dI_{DPLT}/dt = dI_{DPLT}/dT \times dT/dt. \qquad (5)$$

The converted results - dI_{DPLT}/dt as a function of T was displayed in Figure 4 (a).

Figure 2 shows temperature variation of intensity $I(q)$ of SAXS as a function of q, observed at a heating rate of 10 °C/min. In agreement with the previously reported SAXS data observed during slow or stepwise heating, a broad maximum (q_{max}) was observed at approximately q = 0.6 nm^{-1} at room temperature and the maximum shifted toward the lower q side with the increasing the temperature, eventually the maximum disappeared above the melting temperature.

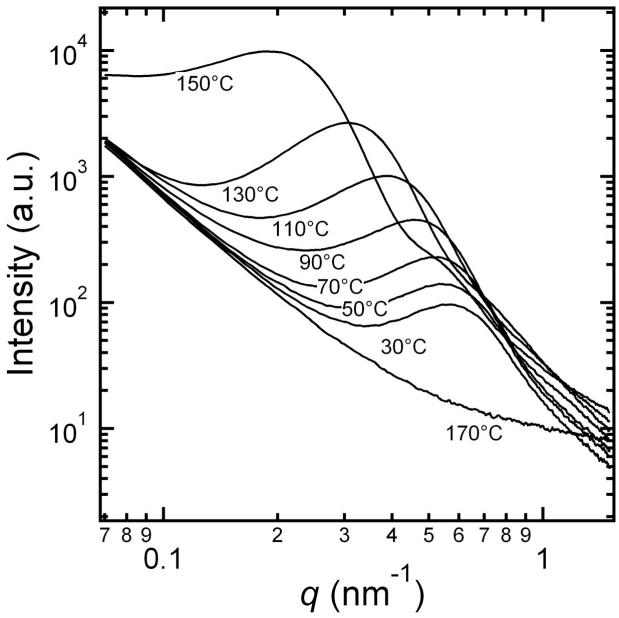

Fig. 2. Temperature variation of SAXS intensity $I(q)$ as a function of q, observed at a heating rate of 10 °C/min.

In general, the scattering profile for a system of dispersed particles is described by a product of the structure factor and the form factor. The maximum in SAXS for the mesophase iPP is assigned to the structure factor caused by the inter-nodular interference. The peak due to the form factor appears in the higher q region than the structure factor's [4]; e.g., a shoulder peak is observed around q = 0.5-0.6 nm^{-1} for the SAXS curve at 150 °C in Figure 2. If both the peaks can be observed, it is useful to estimate the diameter of the nodules D_{nod} accurately. Unfortunately, the requirement cannot always be fulfilled. Instead, approximate value of the average diameter of the nodules D_{nod} is estimated by $2\pi/q_{max}$. The values obtained in this way empirically correspond to those estimated by TEM [11,12].

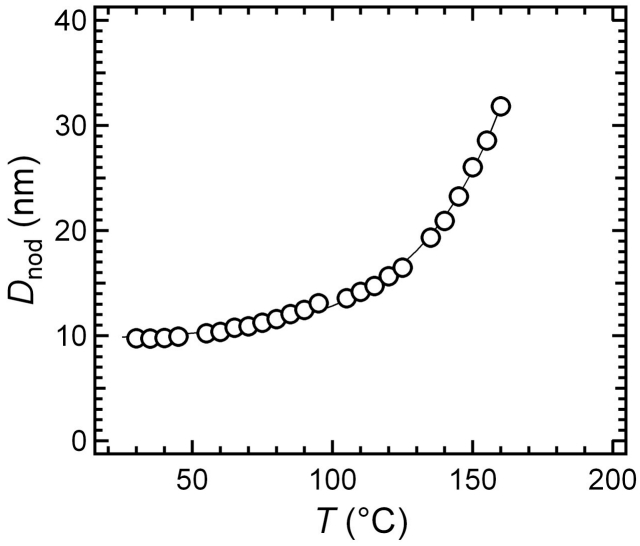

Fig. 3. Diameter of nodule D_{nod} as a function of T at a heating rate of 10 °C/min.

Figure 3 shows the D_{nod} as a function of T. With increasing the temperature, the D_{nod} grew to approximately 30 nm. In nodular systems, temperature dependence of D_{nod} has been explained by the Gibbs-Thomson effects [4]. The D_{nod} as a function of T was also converted into the differential form similarly to equation (4) as follows;

$$dD_{nod}/dt = dD_{nod}/dT \times dT/dt. \qquad (6)$$

The converted results - dD_{nod}/dt as a function of T was displayed in Figure 4 (b).

In our previous paper, the crystallization behavior from the mesophase of iPP was studied using DSC and WAXD during the heating process at a rate of 10 °C/min [10]. There, we obtained the $d(\Delta H)/dT$ and the crystallinity Φ_{cryst} as a function of T. The $d(\Delta H)/dT$ was converted into $d(\Delta H)/dt$ according to equation (4) as mentioned above. The converted results $d(\Delta H)/dt$ as a function of T was displayed in Figure 4 (c). The Φ_{cryst} as a function of T was also converted into the differential form similarly to equation (4) as follows;

$$d\Phi_{cryst}/dt = d\Phi_{cryst}/dT \times dT/dt. \qquad (7)$$

The converted results - $d\Phi_{cryst}/dt$ as a function of T was displayed in Figure 4 (d).

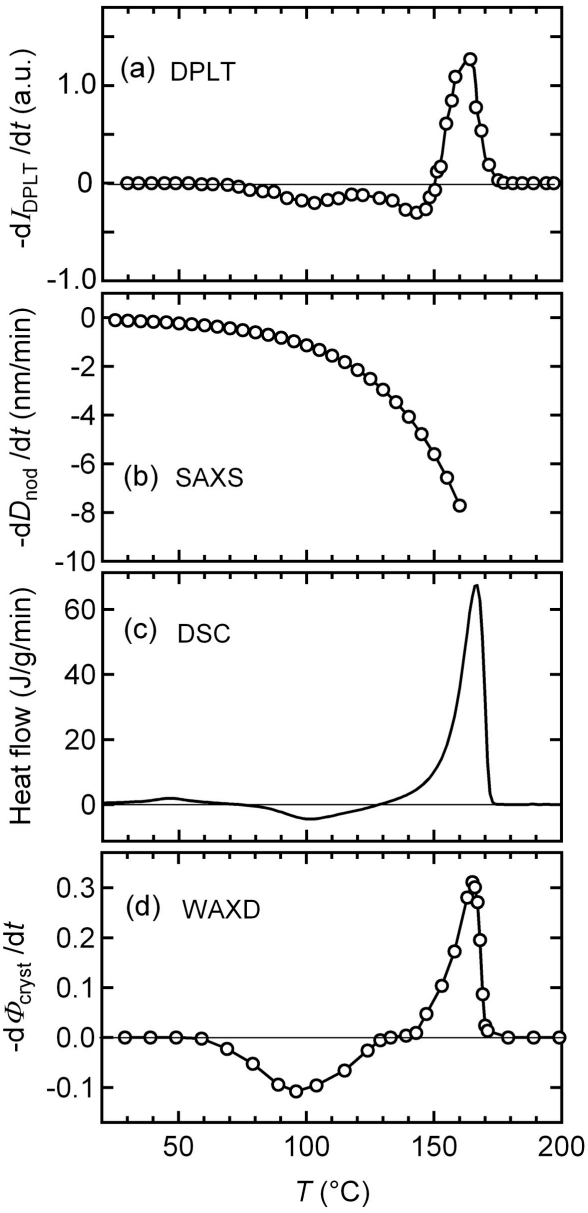

Fig. 4. Methods-weighted rates of structure formations at a rate of 10 °C/min; parts (a), (b), (c), and (d) corresponds to the methods of DPLT, SAXS, DSC, and WAXD, respectively.

Figure 4 shows a full set of the “methods-weighted rates” of structure formations from the mesophase of iPP during the heating process at a rate of 10 °C/min; parts (a), (b), (c), and

(d) corresponds to the methods of DPLT, SAXS, DSC, and WAXD, respectively. Among these methods, the WAXD (Figure 4 (d)) gives the most neutral information in regard to the crystallization and melting, since only the fraction of crystalline phase Φ_{cryst} was extracted from the total WAXD profile by the component analysis [10,20]. A broad minimum around T = 100 °C and a rather sharp maximum T = 165 °C are assigned to the crystallization and the melting of crystal, respectively. This behavior is qualitatively similar to DSC's (Figure 4 (c)), however there are some quantitatively different points as follows. The integrated areas of the crystallization and the melting peaks balance out in the WAXD, whereas the integrated area of the crystallization peak is much smaller than that of the melting in the DSC. The imbalance in the DSC is due to the meta-stability of the mesophase of iPP [10]. Another difference is that only the DSC shows a glass transition-like behavior around 40–50 °C, since the structural measurements like WAXD is less sensitive to the relaxation phenomena. By comparing the DPLT (Figure 4 (a)) to the WAXD (Figure 4 (d)), the shallow minimum around T = 100 °C and a rather sharp maximum T = 165 °C are assigned to the crystallization and the melting of crystal, respectively. It should be noted that only the DPLT shows a specific minimum around 145 °C. To the contrary, the crystallinity is almost constant around 145 °C as is seen in the WAXD (Figure 4 (d)). Therefore, the specific minimum in the DPLT around 145 °C is not ascribed to the crystallization. The SAXS reflects the rate of grain size growth (Figure 4 (b)), independently of the crystallinity. The rate of grain size growth shows progressive increase towards the melting point. Considering this behavior and the detection property of DPLT as was discussed previously (see, equation (3)), the specific minimum around 145 °C in the

DPLT should be assigned to the crystal grain growth. Thus the DPLT is sensitive to not only the crystallization but also the crystal grain growth. These two events did not take place simultaneously but they appeared at well-separated temperature regions (around 100 °C and 145 °C), when iPP was crystallized from the mesophase by heating at a rate of 10 °C/min. In the former region (around 100 °C) it is obvious that the crystallization mainly proceeded by consuming the mesophase (meso-alpha transition); whereas in the latter region (around 145 °C) it is inferred that the crystal grain growth proceeded by partial melting and re-crystallization because the net crystallization rate was close to zero in this temperature region (Figure 4 (d)).

3.2. Heating rate effects on the grain growth rate

Figure 5 shows the heating rate variation of the DPLT measurements, I_{DPLT} as a function of T, for the crystallization of iPP from the mesophase. In order to avoid overlapping, representative plots were displayed. These I_{DPLT} plots for different heating rates, except for 124 °C/min, showed qualitatively similar behavior to the one for 10 °C/min as was previously shown in Figure 1; I_{DPLT} increased showing two steeply increasing regions. The I_{DPLT} plot for 124 °C/min does not show the second steep increase. Further discussion on the heating rate effects for the DPLT is given in the differential form as follows.

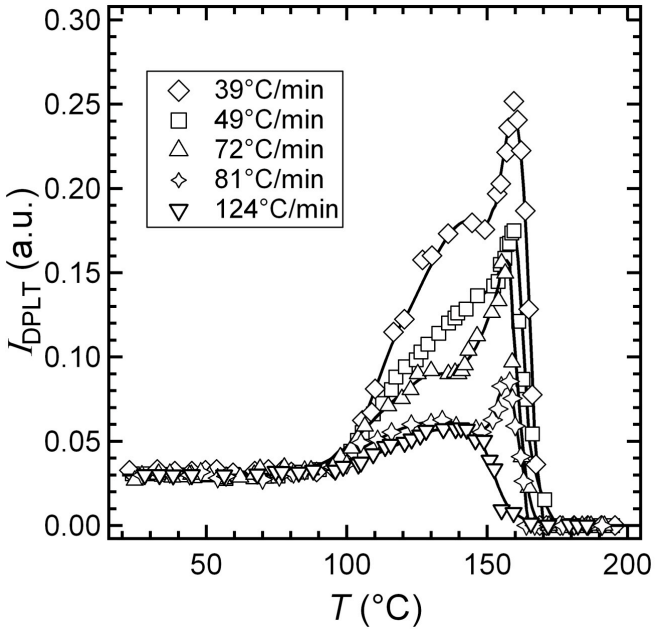

Fig. 5. Heating rate variation of DPLT intensity I_{DPLT} as a function of temperature T.

Figure 6 shows the heating rate variation of - dI_{DPLT}/dt as a function of T. In the differential form of the DPLT, the characteristic of the crystallization of iPP from the mesophase is readable; the first steep increase in the I_{DPLT} plots (Figure 5) appears as a broad minimum around 100–120 °C in - dI_{DPLT}/dt (Figure 6) similarly to the crystallization peak in DSC and WAXD (Figure 4 (c) and (d)), and the second steep increase due to the crystal grain growth appears as a sharp minimum at a higher temperature region around 145–160 °C. With increasing the heating rate, the second minimum became more conspicuous (Figure 6 (b) and (c)). In concert with the sharpening of the second minimum, a new maximum, which is small but a positive value, appeared between the first and second minimum.

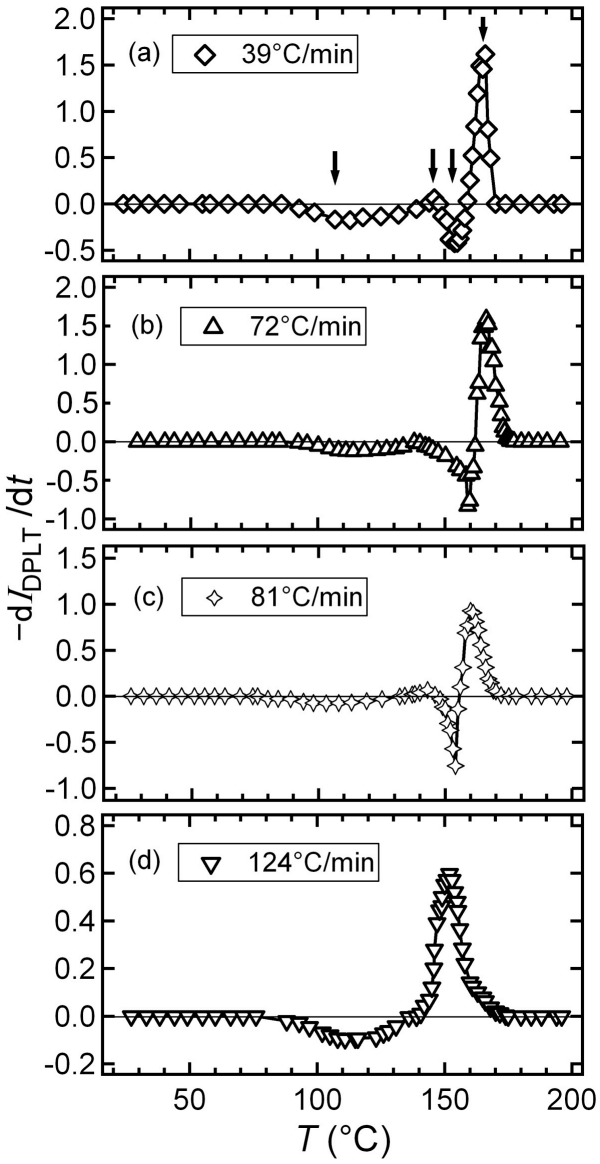

Fig. 6. Heating rate variation of DPLT in differential form - dI_{DPLT}/dt as a function of temperature T.

Considering the detection property of the DPLT and the definition of the - dI_{DPLT}/dt, the positive value means dissolution of a certain structure. Therefore, the appearance of this

maximum together with the succeeding sharp minimum strongly suggests the partial melting and re-crystallization for the mechanism of crystal grain growth. Another important feature is that the second minimum disappeared when the heating rate was too high (Figure 6 (d)). This means that too fast heating prevents the crystal grain growth. Because again the low heating does not much promote the second minimum as was seen in Figure 4 (a), there should be an optimal heating rate favorable for the crystal grain growth.

Figure 7 shows the depth of the second minimum $[- dI_{DPLT}/dt]_{min}$ as a function of the heating rate. Although the plots of $[- dI_{DPLT}/dt]_{min}$ somewhat scatter, there is certainly a maximum around 60–80 °C/min. Present result is significant in order to optimize the heating rate. During the heating process of the mesophase iPP, the crystallization starts at considerably low temperature around 50–60 °C (Figure 4 (d)), which is just above the glass transition-like temperature located around 40–50 °C (Figure 4 (c)). When the heating rate is relatively small, effectively longer aging time is available in the low temperature region. Therefore, the crystallization is promoted in the low temperature region, although the crystallites are cellulated into nodules. In the meantime, the growth in nodule size is not yet conspicuous around 50–60 °C (Figure 4 (b)). If once nodules are thermally stabilized by the crystallization, they are relatively hard to merge into the larger size, in comparison to the less stabilized case. In other words, relatively large heating rate should promote the growth rate of the nodule size.

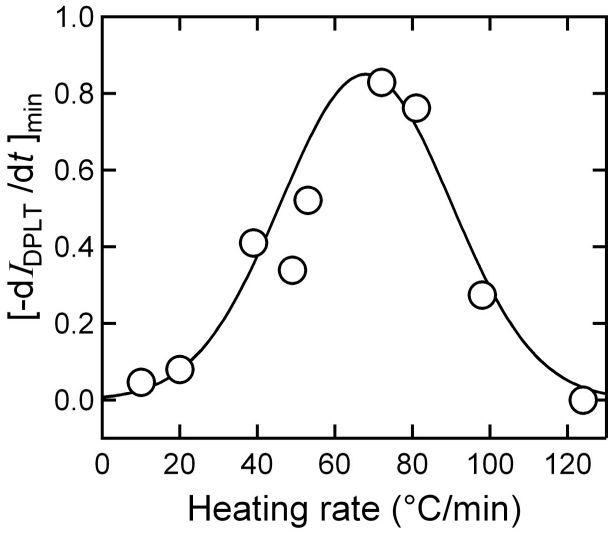

Fig. 7. Depth of the second minimum in differential form of DPLT [- $dI_{DPLT}/dt]_{min}$ as a function of the heating rate.

Figure 8 shows the heating rate variation of the growth rate of nodule - dD_{nod}/dt, as a function of T, for the crystallization of iPP from the mesophase. These data were extracted from the heating rate variation of SAXS measurements, which were performed similarly to Figure 2. At every heating rate, - dD_{nod}/dt decreases, *i.e.*, the growth rate increases, with increasing the temperature until the melting. In the temperature region below 130 °C, the growth rate curves moved to the lower with increasing the heating rate. Namely, the grain growth is accelerated with increasing the heating rate at least in this temperature region. This trend is also valid in the temperature region above 130 °C except for the case of 64 °C/min. It should be noted that, the growth rate curve of 64 °C/min shows conspicuously large negative value, namely, the grain growth is very much accelerated in the temperature region above

130 °C. This behavior (SAXS) is consistent with the discussion for the heating rate effect on the DPLT measurements.

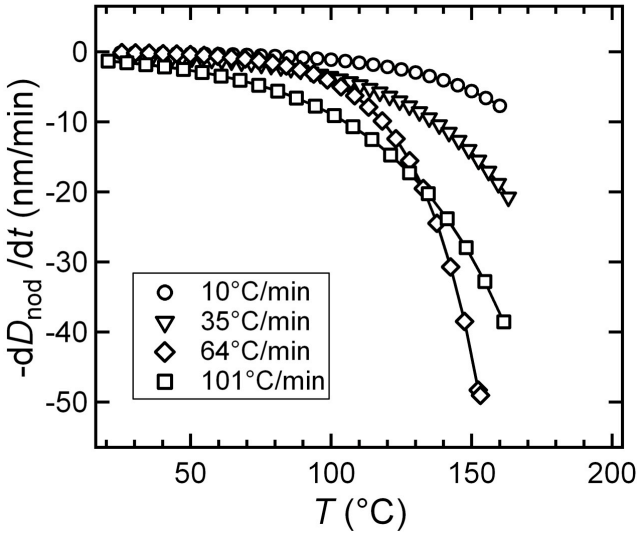

Fig. 8. Heating rate variation of the growth rate of nodule - dD_{nod}/dt, as a function of T.

4. Conclusion

The effectiveness of an application of the de-polarized light transmission (DPLT) method to the crystallization of iPP from the mesophase has been demonstrated. This is due to the merit of sensitive behavior of the DPLT as was mentioned in section 2.3. However, by contraries, the DPLT has a limit of application for the system, e.g., birefringent particles having large domain size (> submicron). For such system, de-polarized light scattering, i.e., Hv light scattering [22], may become an effective step. In the present study an optimal condition in regard to the heating rate was successfully obtained by utilizing the DPLT

method in order to accelerate the crystal grain growth. However, some parameters, such as the isothermal temperature and the period to anneal subsequent to the heating at the specific rate, are left to be scanned in order to optimize the total conditions obtaining the “bamboo leaf-like (BL)” crystal of several tens micron in size, which is one of the ultimate cases of the large size of crystal grain.

References

[1] Norton DR, Keller A. Polymer 1985;26:704–716.

[2] Nakamura K, Shimizu S, Umemoto S, Thierry A, Lotz B, Okui N. Polym J 2008;40:915–922.

[3] Nishida K, Konishi T, Kanaya T, Kaji K. Polymer 2004;45:1433–1437.

[4] Konishi T, Nishida K, Kanaya T. Macromolecules 2006;39:8035–8040.

[5] Gradys A, Sajkiewicz P, Minakov AA, Adamovsky S, Schick C, Hashimoto T, Saijo K. Mater Sci Eng A 2005; 413–414:442–446.

[6] Nishida K, Okada K, Asakawa H, Matsuba G, Ito K, Kanaya T, Kaji K. Polym J 2012;44:95–101.

[7] Miller RL. Polymer 1960;1:135–143.

[8] Turner-Jones A, Aizlewood JM, Beckett DR. Makromol Chem 1964;75: 134–158.

[9] Natta G. SPE J 1959;15:373–382.

[10] Asakawa H, Nishida K, Matsuba G, Kanaya T, Ogawa H. J Phys: Conf Ser 2011;272:[012024-1] – [012024-4].

[11] Hsu CC, Geil PH, Miyaji H, Asai K, J Polym Sci Part B: Polym Phys 1986;24:2379–2401.

[12] Ogawa T, Miyaji H, Asai K. J Phys Soc Jpn 1985;54:3668–3670.

[13] Zia Q, Androsch R, Radusch HJ, Piccarolo S. Polymer 2006;47:8136–8172.

[14] Zia Q. Radusch HJ, Androsch R. Polymer 2007;48:3504–3511.

[15] Androsch R. Macromolecules 2008;41:533–535.

[16] Alberola N, Fugier M, Petit D, Filon B. J Mater Sci 1995;30:1187–1195.

[17] Mileva D, Androsch R, Zhuravlev E, Schick C. Macromolecules 2009;42:7275–7278.

[18] Misztal-Faraj B, Sajkiewicz P, Savytskyy H, Bonchyk O, Gradys A, Ziabicki A. Polym Test 2009;28:36–41.

[19] Su CH, Jeng U, Chen SH, Lin SJ, Wu WR, Chuang WT, Tsau JC, Su AC. Macromolecules 2009;42:6656–6664

[20] Konishi T, Nishida K, Kanaya T, Kaji K. Macromolecules 2005;38:8749–8754.

[21] Nishida K, Ogawa H, Matsuba G, Konishi T, Kanaya T. J Appl Cryst 2008;41:723–728.

[22] Stein RS, Rhodes MB. J Appl Phys 1960;31:1873-1884.